

Controlled Dual Release Study of Curcumin and a 4-Aminoquinoline Analog from Gum Acacia Containing Hydrogels

Blessing Aderibigbe,¹ Emmanuel Sadiku,² Jarugala Jayaramudu,^{2,3} Suprakas Sinha Ray^{3,4}

¹Department of Chemistry, University of Fort Hare, Alice Campus, South Africa

²Department of Chemical, Metallurgical and Material Engineering, Tshwane University of Technology, Pretoria, South Africa

³DST/CSIR National Centre for Nanostructured Materials, Council for Scientific and Industrial Research, Pretoria 0001, South Africa

⁴Department of Applied Chemistry, University of Johannesburg, Doornfontein 2028, Johannesburg, South Africa

Correspondence to: B. Aderibigbe (E-mail: blessingaderibigbe@gmail.com)

ABSTRACT: The potential of gum acacia containing hydrogels as controlled dual-drug delivery systems for antiprotozoal agents was investigated. 4-Aminoquinoline analog and curcumin were selected as model drugs because they exhibit antiprotozoal activity. The maximum release time was greater for curcumin than for the 4-aminoquinoline analog at 37°C, thereby enabling the active ingredients to work over different periods of time. 4-Aminoquinoline analog exhibited a short term release profile while curcumin exhibited a sustained and long term release profile. The release profiles of the drugs were found to be influenced by the degree of crosslinking of the hydrogel network with gum acacia. The release profiles were analyzed using a power law equation proposed by Peppas. The release mechanism of the 4-aminoquinoline was found to be anomalous transport while that of curcumin was quasi-Fickian diffusion mechanism in all the hydrogel networks according to the release exponent. The preliminary results suggest that these systems are potential dual-drug delivery system for antiprotozoal agents with different pharmacokinetics. © 2014 Wiley Periodicals, Inc. *J. Appl. Polym. Sci.* **2015**, *132*, 41613.

KEYWORDS: 4-aminoquinoline; antimalarial; curcumin; gum acacia; hydrogel; kinetic release profile

Received 9 June 2014; accepted 8 October 2014

DOI: 10.1002/app.41613

INTRODUCTION

Dual-drug delivery systems that can control the release behaviors of multiple drugs have recently become an attractive route for enhanced therapeutic effects. Different types of systems such as hydrogels,¹ lipids,² and polymer–drug conjugates^{3–5} have been designed for dual-drug delivery. This study will be focused on the application of hydrogels for dual-drug delivery. Hydrogel is a three-dimensional macromolecular network that has porous structure that permits the loading and release of drugs. The porous structure can be tuned by increasing or decreasing the degree of cross linking of the gel matrix. The degree of cross linking of hydrogel matrix affects its degree of swelling in aqueous medium. They are hydrophilic, biocompatible, and these properties have made them useful for biomedical applications.⁶ They are used for wound dressing,⁷ regenerating tissues and organs,^{8,9} colon specific drug delivery,¹⁰ and for sustained drug delivery systems.¹¹

Natural polymers containing hydrogels have attracted special interests because of their biocompatibility, biodegradability,

hydrophilic, nontoxic characteristics, and hence they are important in biomedical applications.¹² Gum acacia is a natural occurring polymer and it is built from (1 → 3) and (1 → 6)-linked β -D-galactopyranosyl units along with (1 → 6)-linked β -D-glucopyranosyluronic acid units. The side branch contains α -L-rhamnopyranose, β -D-glucuronic acid, β -D-galactopyranose, and α -L-arabinofuranosyl units with (1 → 3), (1 → 4), and (1 → 6) glycosidic linkages.¹³ It is biodegradable, readily available, nontoxic, environmentally friendly, pH stable, and soluble in water.¹⁴ There are several research reports on the biomedical applications of gum acacia. Raghavendra et al. reported the preparation, characterization of biocomposites containing GA with good antibacterial activity against *E. coli*.¹⁵ In a research conducted by Paulino et al., smart hydrogels that exhibit controlled release mechanism were prepared from gum acacia.¹⁶ In another research report by Juby et al., the presence of gum acacia in polyvinylalcohol/gum acacia crosslinked hydrogels loaded with silver nanoparticles was found to influence the degree of swelling of the hydrogels.¹⁷ In a report by Kaith and Ranjta,

Additional Supporting Information may be found in the online version of this article.

© 2014 Wiley Periodicals, Inc.

gum acacia based hydrogels prepared were pH sensitive.¹⁸ In a research report by Santos et al., crosslinked gum acacia-based hydrogels exhibited low degree of swelling in medium of low pH and were found to possess great potential for colon-specific drug delivery systems.¹⁹ In another research report, gum acacia-based hydrogels were found to exhibit high degree of swelling.²⁰ In a research report by Han et al., vaginal hydrogel rings composed of gum acacia exhibited sustained release of nonhormonal contraceptives and anti-HIV agents.²¹ Fathollahipur et al. prepared gum acacia crosslinked hydrogels for wound dressing and were found to release antibiotics at a controlled rate.²²

The drugs under investigation in this study exhibit antiprotozoal activity. A life-threatening disease that is caused by protozoan parasite is malaria. The parasite responsible for this infection is Plasmodium and four different species of plasmodium are responsible for malaria, namely: *P. falciparum*, *P. malariae*, *P. ovale*, and *P. vivax*.²³ The most severe form of malaria is caused by *P. falciparum* and it has developed resistance to nearly all the current antimalarial drugs in use. Until recently, chloroquine a 4-aminoquinoline compound was the most effective drug for treatment of malaria. It acts by binding to the free heme molecules which originate from the degradation of hemoglobin inside the acidic food vacuoles of parasites. This binding hinders the crystallization of hemozoin molecules resulting in the accumulation of heme inside the vacuole to high toxic levels which in turn, leads to parasitic death.²⁴ The cause of chloroquine resistance is believed to be due to alterations in membrane-associated transport processes resulting in a reduced uptake of the drug into the parasite and/or an increased efflux of the drug out of the parasite.²⁴ And because of the drug resistance problem associated with most antimalaria drugs, malaria is treated by a combination of antimalaria drugs with different mechanisms of action. Report has proved that this usually results in high cure rates thereby preventing the onset of drug resistance.²³

The main challenge with combination therapy is the ability to control the release behavior of the individual drug. This usually results in significant decline in renal function and increased toxicity if the pharmacokinetics of the drugs is not well understood.²⁵ There is very little research reports on the design and applications of dual-drug delivery systems for antimalaria drugs.

The rationale for this study is to demonstrate the dual-drug delivery ability of hydrogels containing gum acacia whereby the drugs are allowed to work over different periods of time. This release mechanism has a potential of preventing the onset of drug resistance which is common with the currently used antimalaria drugs. In this present study, gum acacia based hydrogels were prepared by simultaneous redox cross-linked polymerization. The hydrogels were encapsulated with *N*-(7-chloroquinolin-4-yl)propane-1,3-diamine, a 4-aminoquinoline analog of chloroquine and curcumin which both exhibit cytotoxic effect against *P. falciparum*.²⁶ The release profiles of the drugs from the hydrogels were monitored by UV-vis spectroscopy at pH 7.4 (simulating blood pH). The hydrogels were further characterized by Fourier transform infrared spectroscopy (FTIR), scanning electron microscope (SEM), thermo gravimetric analysis (TGA), and X-ray diffraction (XRD).

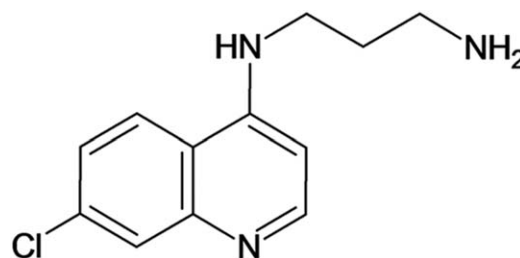


Figure 1. Structure of *N*-(7-chloroquinolin-4-yl)propane-1,3-diamine.

EXPERIMENTAL

Materials

N,N'-Methylenebisacrylamide (MBA) and acrylamide (AM) were obtained from Fluka (South Africa). Gum acacia was obtained from Hopkins and Williams Chemicals. Ammonium persulfate (APS) was purchased from S. D. Fine Company. Distilled water was used for the preparation of the hydrogels.

Synthesis of *N*-(7-chloroquinolin-4-yl)propane-1,3-diamine

N-(7-Chloroquinolin-4-yl)propane-1,3-diamine [Figure 1(a)], a 4-aminoquinoline analog was synthesized by amination reaction of 4,7-dichloroquinoline with neat 1,3-diaminopropane. A mixture of 4,7-dichloroquinoline (1 g, 5.05 mmol) and 1,3-diaminopropane (1.68 g, 22.70 mmol) was heated with reflux for 8 h with continuous stirring and then allowed to cool, after which the resultant solution was diluted with dichloromethane (20 mL) and the mixture was washed with NaOH solution (1 M, 20 mL) and brine (10 mL). An aqueous layer, organic layer, and a coarse white particulate precipitate were obtained. The organic layer was collected and dried over anhydrous sodium sulphate, filtered and then concentrated on a roti-evaporator in order to obtain white solids (Figure 1). The solids were then recrystallized from propylol to afford three crops (1.02 g, 86% yield).^{27,28} The compound was characterized by ¹H-NMR and FTIR to confirm the isolation of the compound.

¹H-NMR (400 MHz, CH₃OD) δ/ppm: 8.35–8.32 (d, 1 H, 6 Hz, Aromatic proton); 8.08–8.05 (d, 1 H, 6 Hz, Aromatic proton); 7.76–7.75 (d, 1 H, Aromatic proton); 7.39–7.36 (dd, 1 H, Aromatic proton); 6.53–6.52 (d, 1 H, 6 Hz, Aromatic proton); 3.512–3.39 (m, 2 H, CH₂); 2.81–2.77 (t, *J* = 12 Hz, 2 H, CH₂NH₂); 1.95–1.84 (dt, 2 H, CH₂) (Supporting Information Figure S1).

Preparation of Gum Acacia Hydrogel Encapsulated with *N*-(7-Chloroquinolin-4-yl)propane-1,3-diamine

The drug encapsulated hydrogels were prepared by dissolving gum acacia in 3 mL of 0.05M of sodium hydroxide solution followed by addition of acrylamide (1 g) and MBA solution (1 mL). The mixture was thoroughly stirred so as to obtain a homogenous mixture before the addition of *N*-(7-chloroquinolin-4-yl)propane-1,3-diamine in methanol (1 mL) and APS (1 mL) (Table I). The hydrogels were formed at a temperature between 40 and 60°C. Blank hydrogel was prepared using the same method (as above) without the addition of gum acacia. The hydrogels were dried at ambient temperature for 3 days (Table I).

Preparation of Curcumin Encapsulated Hydrogel

A stock solution of 50 mg of curcumin dissolved in methanol (40 mL) and 40 mL of water was prepared. 10 mL of the stock

Table I. Composition of Hydrogels (1–9)

Hydrogel	MBA (mL)	Acrylamide (g)	APS (mL)	Gum acacia (g)	4-Aminoquinoline (mg)	Curcumin (mg)
1	1	1	1	–	80	3.60
2	1	1	1	0.05	80	4.80
3	1	1	1	0.10	80	–
4	1	1	1	0.15	80	4.38
5	1	1	1	–	–	–
6	1	1	1	0.05	–	–
7	1	1	1	0.10	–	–
8	1	1	1	0.15	–	–
9	1	1	1	0.10	80	4.50

solution was added to each of the hydrogels (1, 2, 4, and 9). The hydrogels were left in the stock solution overnight at ambient temperature, after which they were rinsed with water so as to remove excess curcumin from the surface of the hydrogels. They were left to dry at ambient temperature for 4 days (Table I).

Proton Nuclear Magnetic Resonance Spectroscopy (¹H-NMR). ¹H-NMR analysis of *N*-(7-chloroquinolin-4-yl)propane-1,3-diamine was performed on Bruker 400 MHz NMR spectroscopy. It was performed using CH₃OD solvent.

Fourier Transform Infrared Spectroscopy (FTIR). FTIR analysis was performed on *N*-(7-chloroquinolin-4-yl)propane-1,3-diamine, curcumin, hydrogels (3, 4, and 6) in the wavelength range of 400–4000 cm^{−1}. The FTIR spectroscopy was performed on a Perkin Elmer Spectrum 100 FTIR spectrometer, (USA). It was used to identify the functional groups present on the 4-aminoquinoline analog and curcumin and to indicate the presence of these functionalities in the hydrogels encapsulated with curcumin and the 4-aminoquinoline analog.

Swelling Ratio

Swelling ratio of the hydrogels influences the release mechanism of the drug from the hydrogel. Equilibrium swelling studies of the dried hydrogels were performed at ambient temperature over a period of 24 h. It was performed at pH 7.4 (simulating blood pH). The hydrogels were made to swell in the buffer solution until equilibrium swelling was reached (after 24 h). They were removed and blotted gently with blotting paper to remove the overloaded water on the surface and weighed. The immersion time and drying of the hydrogels were repeated until the masses of the swollen hydrogels were constant. The swelling ratio at equilibrium (ESR) was calculated (Table II) from eq. 1:

$$ESR = \frac{(M_s - M_d)}{M_d} \quad (1)$$

The swelling ratio (SR) measurements for the hydrogels were performed after every 30 min at pH 7.4. After 30 min, the hydrogels were removed from the buffer solution and blotted gently with blotting paper and weighed. This is calculated as (SR) from eq. 2:

$$SR = \frac{M_t - M_d}{M_d} \quad (2)$$

where M_s is the weight of the hydrogel at equilibrium, M_t is the weight of the hydrogel at time t and M_d is the weight of the dry hydrogel before swelling.

Encapsulation Efficiency

The percentage encapsulation efficiencies (EE) was calculated, based on the ratio of amount of curcumin encapsulated onto the hydrogels to the amount used in the loading process. It was determined using UV–visible spectroscopy (Perkin Elmer LAMDA 750S UV/VIS Spectrometer) at a wavelength of 428 nm. The percentage encapsulation efficiencies of the hydrogels were calculated using eq. 3:

$$EE = \frac{A_1}{A_2} \times 100\% \quad (3)$$

where A_1 is the actual amount of curcumin loaded on to the hydrogel and A_2 is the theoretical amount of curcumin loaded on the hydrogel. The EE results are depicted in Table III.

Scanning Electron Microscopy (SEM)

SEM analysis was performed on EOL-JSM 7500F Scanning Electron Microscope (USA). This was used to investigate the surface morphologies of curcumin, *N*-(7-chloroquinolin-4-yl)propane-1,3-diamine, hydrogels (before and after encapsulation with curcumin) and the hydrogel encapsulated with *N*-(7-chloroquinolin-4-yl)propane-1,3-diamine.

X-ray Diffraction (XRD)

XRD was performed using PANalytical X'Pert PRO (USA) on the hydrogels at (Cu K_α radiation, $\lambda = 0.1546$ nm) running at 45 kV and 40 mA. This analysis was performed in order to

Table II. Swelling Ratios for the Hydrogels

Hydrogels	Swelling ratio (mean ± SD)
5	7.15 ± 0.91
6	12.51 ± 0.83
7	10.73 ± 0.90
8	9.67 ± 0.89

Table III. Drug Encapsulation Efficiencies and Kinetic Release Constants of Curcumin from Hydrogels (1, 2, 4, and 9)

Hydrogel	Zero order		Higuchi		Korsmeyer Peppas		Curcumin loading (%)
	R^2	K	R^2	K	R^2	n	
1	0.982	0.01	0.960	0.10	0.996	0.11	26
2	0.999	0.42	0.995	5.53	0.990	0.24	38
4	0.960	0.10	0.920	1.24	0.990	0.45	32
9	0.930	0.25	0.900	3.25	0.980	0.35	34

evaluate the interaction of curcumin and *N*-(7-chloroquinolin-4-yl)propane-1,3-diamine with the hydrogel network.

Thermo Gravimetric Analysis

TGA was used to determine the effect of the degree of crosslinking on the thermal stability of the hydrogel networks. It was performed using the TA-TGA Q500 (USA) at a heating rate of $10^\circ\text{C min}^{-1}$ and at a range of $40\text{--}700^\circ\text{C}$ under a constant nitrogen flow of 60 mL min^{-1} .

In Vitro Release Studies

An *in vitro* drug release study was performed by placing the hydrogel encapsulated with curcumin and 4-aminoquinoline in

a 30 mL of 7.4 buffer solution at 37°C . A shaker BS-06 (Lab Companion) was used at 100 RPM. The release profiles for curcumin and 4-aminoquinoline were obtained using UV-visible spectroscopy. The release study was performed over a period of 24 h by collecting 4 mL of the sample solution and replacing it with equivalent amount of buffer solution. *N*-(7-chloroquinolin-4-yl)propane-1,3-diamine release from the hydrogels to the buffer solution was determined by measuring the absorbance value at 329 nm while curcumin release was performed at an absorbance value of 428 nm. The percentage cumulative release (CR) of curcumin and 4-aminoquinoline analog was calculated using eq. 4.

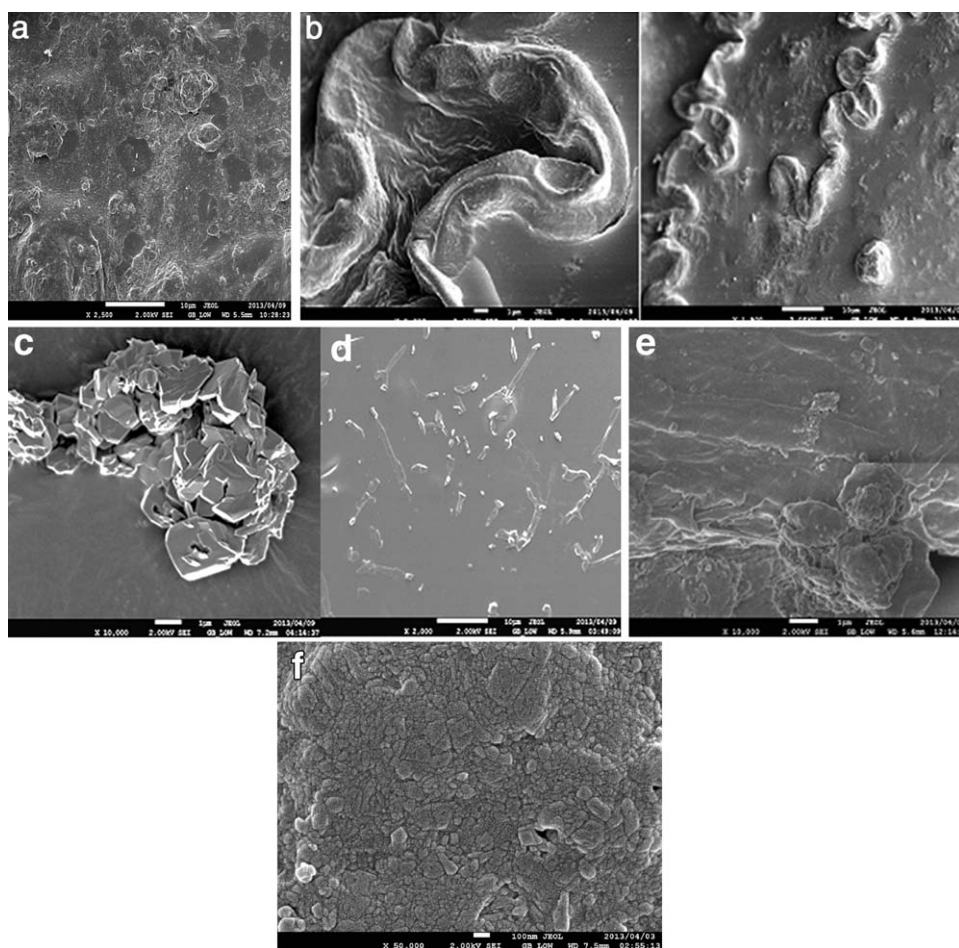


Figure 2. a: SEM image of blank hydrogel 5, b: SEM image of hydrogel 8, c: SEM image of *N*-(7-chloroquinolin-4-yl)propane-1,3-diamine, d: SEM image of hydrogel 3 loaded with *N*-(7-chloroquinolin-4-yl)propane-1,3-diamine, e: SEM image of hydrogel 2 loaded with *N*-(7-chloroquinolin-4-yl)propane-1,3-diamine and curcumin, f: SEM image of curcumin.

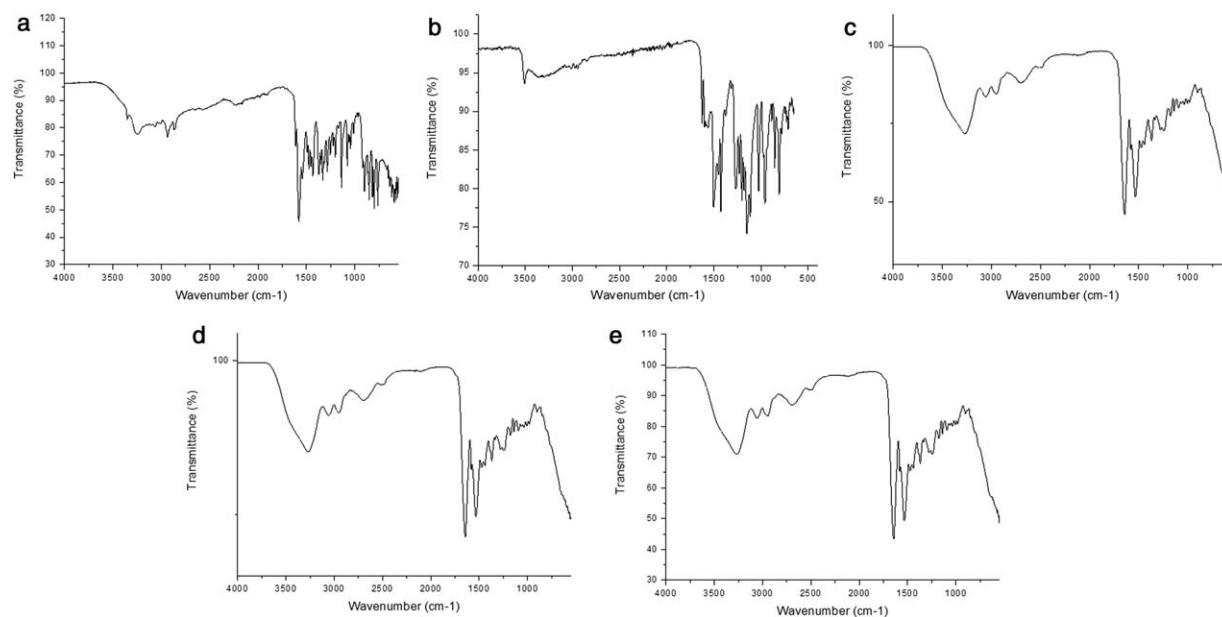


Figure 3. a: FTIR spectrum of *N*-(7-chloroquinolin-4-yl)propane-1,3-diamine, b: FTIR spectrum for curcumin, c: FTIR spectrum of hydrogel 6, d: FTIR spectrum of hydrogel 3 loaded with *N*-(7-chloroquinolin-4-yl)propane-1,3-diamine, e: FTIR spectrum of hydrogel 4 loaded with *N*-(7-chloroquinolin-4-yl)propane-1,3-diamine and curcumin.

$$\%CR = \frac{I_i}{I_f} \times 100 \quad (4)$$

where I_i and I_f are the initial amount and cumulative amount of curcumin and 4-aminoquinoline released at time t .

RESULTS AND DISCUSSION

Synthesis of *N*-(7-Chloroquinolin-4-yl)propane-1,3-diamine

N-(7-Chloroquinolin-4-yl)propane-1,3-diamine was synthesized according to a modification of De's method.²⁷ White solids with a relatively excellent yield of 86% of high purity was isolated. NMR analysis was performed using CH₃OD as solvent. ¹H-NMR spectrum showed signals for the aromatic protons at 8.35–8.32, 8.08–8.05, 7.76–7.75, 7.39–7.36, and 6.53–6.51 ppm. Further analysis was performed on the compound using FTIR spectroscopy, which confirmed the isolated compound [Figure 1(b)].

SEM Analysis

SEM analysis was performed so as to evaluate the surface morphologies of *N*-(7-chloroquinolin-4-yl)propane-1,3-diamine, curcumin, hydrogel encapsulated with curcumin and *N*-(7-chloroquinolin-4-yl)propane-1,3-diamine, blank hydrogel, gum acacia containing hydrogel, and gum acacia containing hydrogel encapsulated with *N*-(7-chloroquinolin-4-yl)propane-1,3-diamine. The morphology of the blank hydrogel 5 was irregular and slightly coarse with spherical morphology [Figure 2(a)]. Gum acacia containing hydrogel 8 exhibited folded topologies which are as a result of the presence of gum acacia [Figure 2(b)]. *N*-(7-chloroquinolin-4-yl)propane-1,3-diamine exhibited a cluster of block-like morphology resulting from the crystalline nature of the compound [Figure 2(c)]. Hydrogel containing gum acacia 3 encapsulated with *N*-(7-chloroquinolin-4-yl)propane-1,3-diamine exhibited dispersed block-shaped

morphologies which is attributed to *N*-(7-chloroquinolin-4-yl)propane-1,3-diamine encapsulation onto the hydrogel [Figure 2(d)]. Hydrogel 2 encapsulated with curcumin and *N*-(7-chloroquinolin-4-yl)propane-1,3-diamine displayed a combination of a folded topologies, spherical and block-like morphologies [Figure 2(e)]. The folded morphology is as a result of the presence of gum acacia and the spherical and block-shaped morphologies is attributed to the encapsulated curcumin and *N*-(7-chloroquinolin-4-yl)propane-1,3-diamine, respectively [Figure 2(e)]. The morphology of curcumin exhibited coarse surface with spherical morphology [Figure 2(f)].

FTIR Analysis

The FTIR spectrum of *N*-(7-chloroquinolin-4-yl)propane-1,3-diamine displayed N–H stretching at 3300 cm⁻¹, aromatic C=C stretching at 1577 cm⁻¹, C–N stretching at 1330 cm⁻¹, C–H stretching at 2850 cm⁻¹, thereby confirming the isolated compound [Figure 3(a)]. This was in agreement with FTIR spectrum by Rojas and Kouznetsov which further confirmed the successful isolation of the 4-aminoquinoline compound.²⁹

The FTIR spectrum of curcumin exhibited characteristic O–H stretching of the phenol group at 3501 cm⁻¹, CH stretching, intermolecular H-bond stretching at 3303 cm⁻¹, CH stretching of the OCH₃ was visible at 2958 cm⁻¹. Inplane bending of aromatic (CCC, CCH), enolic (COH), and the CH inplane bending due to CH₂ peak was visible at 1428 cm⁻¹, inplane bending of aromatic CCH, skeletal CCH was visible 1152 cm⁻¹, C=O stretching and in plane of CCH was visible at 962 cm⁻¹ [Figure 3(b)].³⁰

FTIR spectrum of gum acacia containing hydrogel 6 displayed sharp amide peaks for C=O at 1638 cm⁻¹, C–H stretching at 2933 cm⁻¹, N–H at 3384 cm⁻¹, characteristic glycosidic linkage

bond (C–O–C) was evident between 1160 and 1139 cm^{-1} and C–OH stretching of gum acacia was visible at 1080 cm^{-1} , thereby signifying the presence of gum acacia in the hydrogel [Figure 3(c)]. The characteristic peak for GA in hydrogels cross linked with GA at 1160–1139 cm^{-1} and 1080 was also reported by Juby et al., Dostelek et al., and Rao et al.^{17,20,31} This further confirmed the successful crosslinking of gum acacia with the polymer chain.

FTIR spectrum of hydrogel 3 encapsulated with *N*-(7-chloroquinolin-4-yl)propane-1,3-diamine displayed characteristic peaks for N–H stretching at 3389 cm^{-1} , aromatic C=C stretching at 1578 cm^{-1} , C–N stretching at 1333 cm^{-1} , C–H stretching at 2852 cm^{-1} and glycosidic linkage bond (C–O–C) was evident between 1160 and 1139 cm^{-1} , therefore confirming the successful encapsulation of *N*-(7-chloroquinolin-4-yl)propane-1,3-diamine and the presence of gum acacia [Figure 3(d)].

The FTIR spectrum for hydrogel 4 encapsulated with curcumin and *N*-(7-chloroquinolin-4-yl)propane-1,3-diamine exhibited absorption peaks of curcumin at 2960 cm^{-1} for CH stretching of OCH_3 , in-plane bending of aromatic (CCC, CCH), enolic (COH), CH in plane bending due to CH_2 peak was visible at 1427 cm^{-1} , inplane bending of aromatic CCH, skeletal CCH was visible 1154 cm^{-1} , C=O stretching and in plane of CCH was visible at 966 cm^{-1} . Absorption peaks of *N*-(7-chloroquinolin-4-yl)propane-1,3-diamine were visible for N–H stretching at 3350 cm^{-1} , aromatic C=C stretching at 1576 cm^{-1} , C–N stretching at 1333 cm^{-1} , therefore confirming the successful entrapment of curcumin and *N*-(7-chloroquinolin-4-yl)propane-1,3-diamine on to the hydrogel [Figure 3(e)].

XRD Analysis

XRD was used to evaluate the interaction of *N*-(7-chloroquinolin-4-yl)propane-1,3-diamine and curcumin with the polymer chain. The diffraction pattern for the *N*-(7-chloroquinolin-4-yl)propane-1,3-diamine was sharp due to its crystalline nature, whereas the hydrogels diffraction pattern were found to be very broad and diffuse. The characteristic diffraction peaks of *N*-(7-chloroquinolin-4-yl)propane-1,3-diamine were visible at $2\theta = 25.22, 25.30, 25.36, 25.41, 25.86,$ and 43.29° , respectively [Figure 4(a)]. These peaks were present but broad and diffuse in hydrogels 2 and 3 loaded with *N*-(7-chloroquinolin-4-yl)propane-1,3-diamine. The characteristic diffraction peaks of curcumin were visible at $2\theta = 8.83, 12.14, 14.14, 14.43, 17.22,$ and 25.56° , respectively [Figure 4(b)]. These peaks were present in the hydrogel 2 loaded with curcumin but they were broad with low intensity because of the amorphous nature of the hydrogels. The XRD graphs indicated the amorphous nature of the hydrogel and the molecular dispersion of the drugs in the hydrogel network. It further indicated that there was no interaction between the drugs and the hydrogel network.

TGA

TGA was used to evaluate the stability of the drugs, the drug encapsulated hydrogels and the effect of the degree of cross-linking on the thermal stability of the hydrogels network. *N*-(7-chloroquinolin-4-yl)propane-1,3-diamine exhibited the initial weight loss of 6.7% after 80°C as a result of loss of

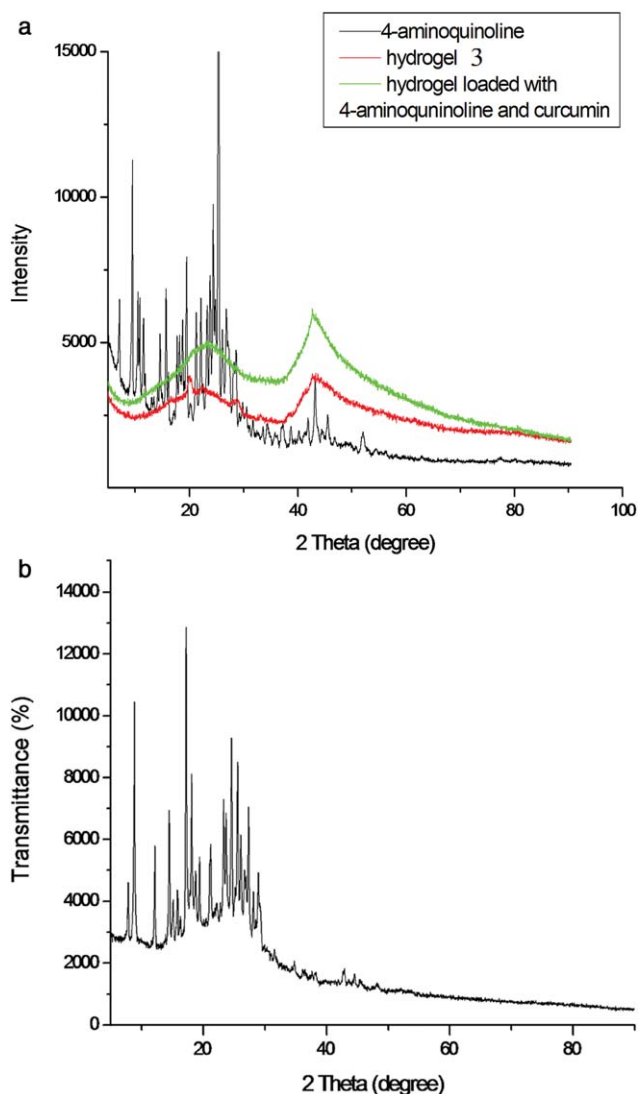


Figure 4. a: XRD graphs of hydrogel 2 loaded with curcumin and *N*-(7-chloroquinolin-4-yl)propane-1,3-diamine, hydrogel 3 loaded with *N*-(7-chloroquinolin-4-yl)propane-1,3-diamine, b: XRD graph of curcumin. [Color figure can be viewed in the online issue, which is available at wileyonlinelibrary.com.]

water molecules, a second weight loss of 60% was observed after 250°C, a third weight loss of 6.7% was evident after 400°C and the final weight loss of 26.6% was found after 600°C. The last weight loss is as a result of the decomposition of the *N*-(7-chloroquinolin-4-yl)propane-1,3-diamine [Figure 5(a)]. Curcumin displayed the first weight loss of 28.6% after 300°C which is attributed to the liberation of moisture in the sample. The second weight loss of 71% was between 320 and 520°C. This last weight loss is due to the decomposition of the curcumin [Figure 5(b)]. Hydrogel 6 displayed a steady weight loss and the initial weight loss of 7.4% was observed after 220°C, a second weight loss of 8.8% occurred after 270°C, a third weight loss of 46% was evident after 410°C and a final weight loss of 37% was recorded between 420 and 550°C [Figure 5(c)]. Hydrogel 5 exhibited a rapid weight loss of 35.7% between 100 and 370°C, a weight

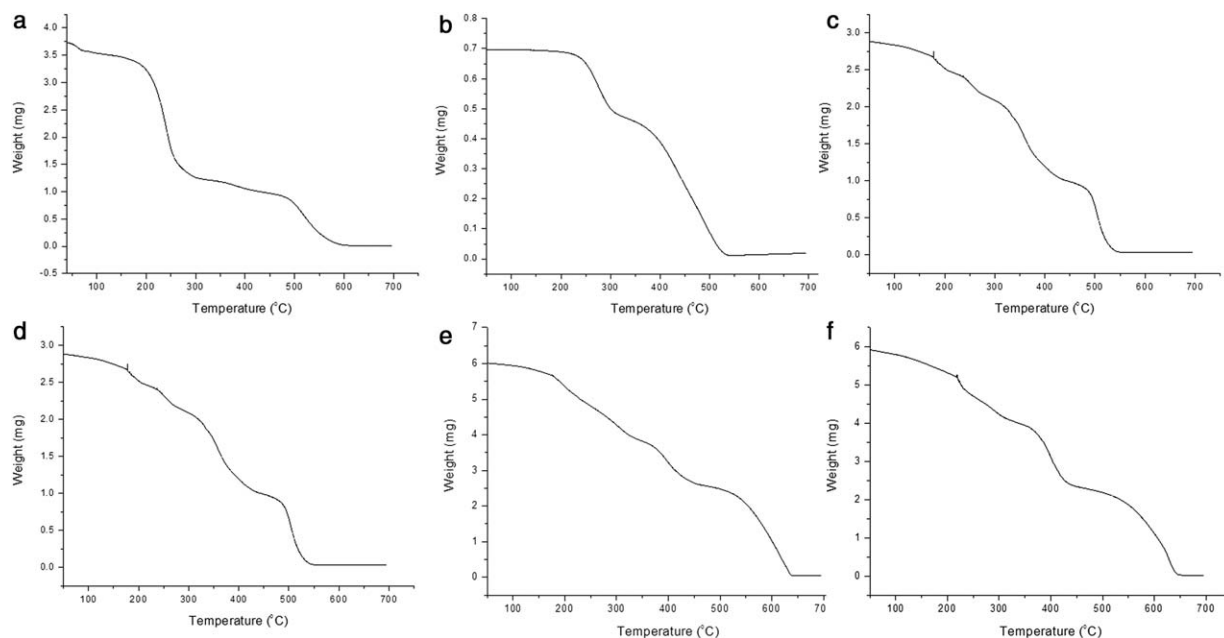


Figure 5. a: TGA graph of *N*-(7-chloroquinolin-4-yl)propane-1,3-diamine, b: TGA graph of curcumin, c: TGA graph of hydrogel 6, d: TGA graph of hydrogel 5, e: TGA graph of hydrogel 3, f: TGA graph of hydrogel 2 loaded with *N*-(7-chloroquinolin-4-yl)propane-1,3-diamine and curcumin.

loss of 29% was visible after 430°C and the final weight loss of 35% was evident up till 650°C which is due to the decomposition of the hydrogel [Figure 5(d)]. Hydrogel 3 initial weight loss of 8.3% was visible after 170°C, a second weight loss of 25% was evident after 330°C, a third weight loss of 20% was recorded after 440°C and the final weight loss of 43% was found after 640°C, which is due to the decomposition of *N*-(7-chloroquinolin-4-yl)propane-1,3-diamine and the hydrogel [Figure 5(e)]. Hydrogel 2 loaded with *N*-(7-chloroquinolin-4-yl)propane-1,3-diamine and curcumin recorded weight losses of 8.3, 15.7, 25, and 41.7% after 225, 325, 425, and 640°C, respectively [Figure 5(f)]. The hydrogel network cross-linked with gum acacia was found to be more thermally stable than the blank hydrogel. The hydrogels containing gum acacia displayed a steady weight loss whereas, the blank hydrogel weight loss was rapid. Hydrogels 2 and 3 encapsulated with the model drugs exhibited a steady weight loss and they were thermally stable. Similar findings on the improved thermal stability of hydrogel cross linked with GA was reported by Kaith and Ranjta.¹⁸ This further confirmed that the addition gum acacia to the hydrogel network enhances its thermal stability.

Swelling Ratio

In this study, the effect of the concentration of gum acacia in the hydrogels on the water sorption ability of the equilibrium hydrogels were evaluated at a pH of 7.4 simulating blood pH. The water sorption capacity of the hydrogels is shown in Table II. At this pH, hydrogel 6 which had the least concentration of gum acacia was found to exhibit the highest swelling ability, whereas hydrogels 7, 8 and 5 exhibited moderate to low swelling abilities, respectively. This observation indicated that the swelling ratio of gum acacia cross-linked hydrogels increased with a decrease in the concentration of gum acacia. When the concentration of gum acacia is low in the hydrogel network, it renders

the network more hydrophilic, due to the hydroxyl and carboxyl group; thereby increasing the degree of water sorption and swelling ratio. Hydrogel 5 (i.e., without gum acacia) exhibited the lowest swelling ability which implies that the addition of natural occurring polymer to hydrogels renders the network more hydrophilic because of the hydroxyl and carboxyl groups in the gum acacia. When the content of the gum acacia was increased from 0.05 to 0.10 and 1.5 g, respectively, the swelling ratio decreased because an increase in the concentration of gum acacia reduced the mesh size and increased the compartment thereby leading to reduced degree of water sorption and reduced swelling ratio.³² The swelling ratios (SR) of the hydrogels was examined after every 30 min and the graph of swelling ratio versus time was obtained [Figure 6(a)]. The hydrogel 6 with the least content was found to swell faster than the other hydrogels. The solvent diffusion and polymer matrix relaxation effect³³ was analyzed by examining the exponent n from eq. 5.

$$\frac{SR_t}{SR_\infty} = Kt^n \quad (5)$$

where K is the diffusion constant of water into the hydrogel network and n is the swelling exponent at time t . When $n = 0.5$, it indicates case I, which is a perfect Fickian process in which the rate of network relaxation is faster than the rate of diffusion. When $n = 1.0$, it indicates case II, which is referred to as a super case transport, where the mobility of the penetrant is faster than the chain relaxation rate and the solvent uptake is directly proportional to time. When $0.5 < n < 1.0$, it indicates that the rate of penetrant mobility and segmental relaxation are comparable.³³ A graph of $\ln(SR)$ versus $\ln t$ was plotted for the initial 60% increase of the mass of the hydrogels at pH 7.4. The swelling exponent n was obtained from the slope of the graph and K was the intercept on the SR axis [Figure 6(b)]. The swelling exponent n was found to be 0.62, 0.65, and 0.66 for

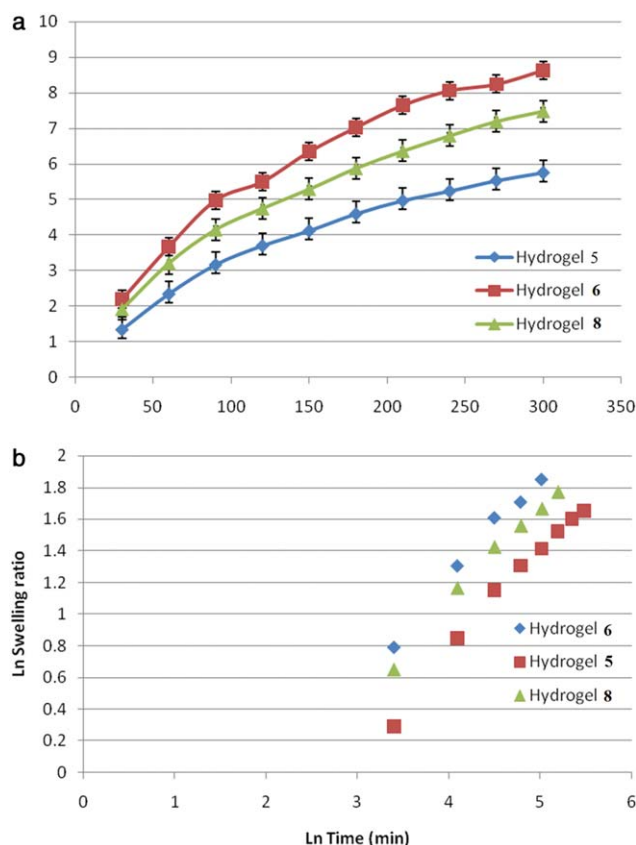


Figure 6. a: A graph of swelling ratio versus time for the hydrogels, b: a graph of \ln swelling ratio versus \ln time for the hydrogels. [Color figure can be viewed in the online issue, which is available at wileyonlinelibrary.com.]

hydrogels 5, 8, and 6 respectively, indicating an anomalous non-Fickian process with a coefficient of correlation between 0.989–0.999, indicating good linearity. This result further confirmed that crosslinking the hydrogel network with gum acacia influenced the degree of water sorption into the hydrogel network. The swelling pattern of the hydrogels were similar to the research report of GA based hydrogel by Juby et al., Kaith et al.^{17,18,34} From previous findings in our research group (unpublished), the gum acacia hydrogels exhibited low swelling abilities at a pH of 1.2 because the carboxylate anions are protonated and as such, anion–anion repulsive forces are eliminated. This finding was consistent with report by Santos et al. and Zohuriaan-Mehr et al. on similar release systems confirming their pH sensitive nature.^{19,35} And based on this finding, this study was performed at a pH of 7.4.

In Vitro Dual-Drug Release

There is very little research report on *in vitro* release studies of antimalarial drugs from dual-drug delivery systems. The currently reported dual-drug delivery systems for antimalarial are polymer–drug conjugates. However, in some of our research reports, polymeric carriers were prepared with selected linkers that are pH sensitive for drug incorporation.^{3–5} Antimalarial agents were incorporated onto the polymeric carriers via selected linkers to form polymer–drug conjugates. Polymer–drug conjugates containing selected linkers were found to be

very active against the chloroquine-sensitive strain of *P. falciparum*.³ These findings brought to light, the potentials of polymer-based drug delivery systems for combination therapy of antimalarial drugs. The percentage encapsulation efficiencies of the antimalarial drugs onto the polymeric carriers was lower than expected and this was attributed to incomplete coupling reactions, steric hindrance, etc.^{3,36} In order to increase the percentage encapsulation of the antimalarial on to polymer-based drug-delivery systems, we were prompted to use hydrogels because of their ability of absorb a large amount of water or biological fluid. In a research report on the application of hydrogel nanoparticles for delivery studies of curcumin, the absorption of curcumin was improved with excellent encapsulation efficiency and prolonged release mechanism.³⁷

Gum acacia containing hydrogels on the other hand has been found to exhibit controlled release mechanism. To the best of our knowledge, there is no report on the application of gum acacia hydrogel for dual-drug delivery. Based on the controlled release mechanism of gum acacia containing hydrogels, we decided to move a step forward by demonstrating the ability of gum acacia containing hydrogels (a polymer-based drug delivery system) to act as dual-drug release system. Hydrogels 1, 2, 4, and 9 with varied concentration of gum acacia were evaluated at pH 7.4 over a period of 24 h. The drugs release profiles were obtained using UV–visible spectroscopy at wavelengths 329 nm for *N*-(7-chloroquinolin-4-yl)propane-1,3-diamine and at 428 nm for curcumin. Both drugs selected exhibit low solubility

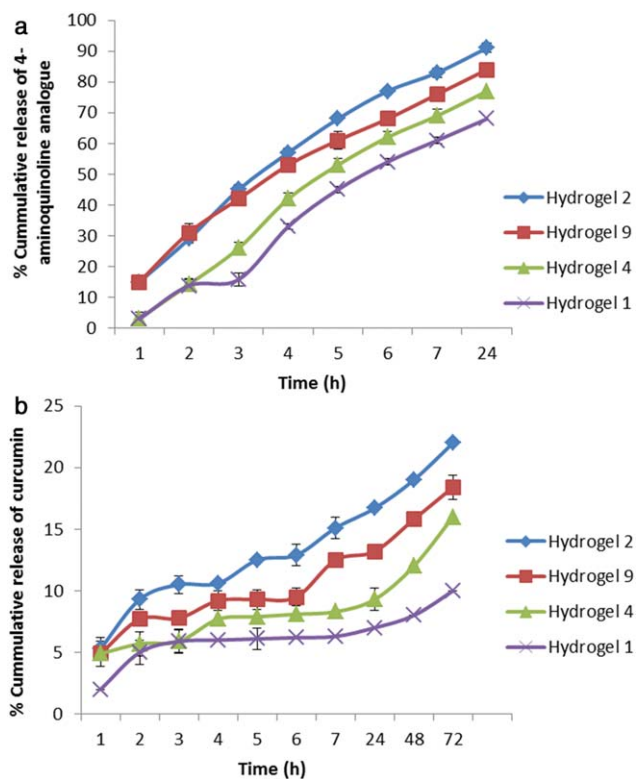


Figure 7. a: A graph of the release profile of *N*-(7-chloroquinolin-4-yl)propane-1,3-diamine from the hydrogels 1, 2, 4, and 9, b: A graph of the release profile of curcumin from hydrogels 1, 2, 4, and 9. [Color figure can be viewed in the online issue, which is available at wileyonlinelibrary.com.]

Table IV. Drug Encapsulation Efficiencies and Kinetic Release Constants of the 4-Aminoquinoline Analog from Hydrogels (1, 2, 4, and 9)

Hydrogel	Zero order		Korsmeyer Peppas	
	R^2	K	R^2	n
1	0.980	9.85	0.970	1.50
2	0.981	11.53	0.999	0.98
4	0.980	10.05	0.988	1.76
9	0.990	11.43	0.993	1.60

in water which made them ideal drugs for this study and they exhibited different release behavior from the hydrogels. Curcumin exhibited a sustained release profile whereas, *N*-(7-chloroquinolin-4-yl)propane-1,3-diamine exhibited a short term release. Hydrogel **6** which exhibited the highest swelling ratio was loaded with both drugs to isolate hydrogel **2**. Hydrogel **2** was found to release both drugs faster than the other hydrogels. Hydrogel **2** released 91% of *N*-(7-chloroquinolin-4-yl)propane-1,3-diamine over a period of 24 h, whereas only 16.7% of curcumin was released over the same period [Figure 7(a,b)]. The percentage encapsulation efficiencies of curcumin onto hydrogels **5**, **6**, **7**, and **8** to isolate hydrogels **1**, **2**, **4**, and **9** were between 26 and 38% (Table III). Hydrogel without gum acacia released 7% of curcumin and 68% of *N*-(7-chloroquinolin-4-yl)propane-1,3-diamine after 24 h. Hydrogel **4** released 9.2% of curcumin and 77% of *N*-(7-chloroquinolin-4-yl)propane-1,3-diamine after 24 h. Hydrogel **9** released 13.2% of curcumin and 84% of *N*-(7-chloroquinolin-4-yl)propane-1,3-diamine after 24 h (Table IV). Gum acacia containing hydrogel **4** with the highest content of gum acacia released the drug slower than other hydrogels containing gum acacia. Hydrogel without gum acacia released the drug slower than all the other hydrogels. The drug release result was in good agreement with the effect of the concentration of gum acacia on the swelling of hydrogel as discussed in the previous section. The result further confirmed the effect of the content of gum acacia in the hydrogel on the rate of drug release from the hydrogels. This finding is similar to the research report by Nishi and Jayakrishnan in which the release of a 8-aminoquinoline from gum acacia containing hydrogel was found to be dependent on the degree of crosslinking.³⁸ To understand the mechanism of release of the drugs from the hydrogels, Peppas³⁹ equations 6 and 7 were used at a temperature of 37°C and at a pH of 7.4.

$$\frac{M_t}{M_\infty} = Kt^n \quad (6)$$

$$\log \frac{M_t}{M_\infty} = n \log t + \log K \quad (7)$$

where M_t is the amount of drug released at time t , M_∞ is the total amount of drug encapsulated on to the hydrogels, K is the kinetic constant, and n is the diffusion or release exponent. A graph of $\log (M_t/M_\infty)$ against $\log t$ of the experimental data was drawn according to eqs. 6 and 7. Diffusion exponent, n was estimated from the linear regression of the graph. According to Peppas equation, when $n=0.5$, it indicates Fickian diffusion, when $0.5 < n < 1$, it indicates anomalous or non-Fickian diffusion which

refers to a combination of diffusion and erosion controlled rate release. If $n = 1$ and above it indicates case 2 relaxation⁴⁰ or super case transport 2. The n value for the 4-aminoquinoline analog was found to be between 0.98 and 1.76 indicating anomalous diffusion. Good linearity indicated that Peppas's release equation is applicable to these systems (Table IV). From the kinetics analysis data for curcumin from the hydrogels, r^2 of the release data closely fitted zero-order and Korsmeyer–Peppas models. The low values of n (<0.5) indicated that the release mechanism of curcumin from all the hydrogel can be described as a quasi-Fickian diffusion mechanism (Table III).

The different release mechanisms for curcumin and the 4-aminoquinoline analog suggest that the hydrogel has a marked influence on their release behavior of the drugs when used in combined delivery. Similar release pattern of two drugs from dual-drug delivery systems have been reported by Castro et al. on dual-drug release of triamterene and aminophylline from poly (*N*-isopropylacrylamide) hydrogels⁴¹ and Wei et al. on dual-drug release study of doxorubicin and aspirin from hydrogel composites.¹ Pearale et al. reported similar finding which involved a combination of fast diffusion controlled kinetics for smaller molecules together with a slow diffusion-controlled kinetics for bigger molecules from a multidrug delivery hydrogel system for spinal cord injury repair.⁴²

To the best of our knowledge, we have reported a first example of dual-drug delivery systems which are based on gum acacia containing hydrogels. These drug delivery systems exhibit some unique properties which are useful for clinical applications such as: easy preparation, control release profile of individual drug which is dependent on the degree of cross-linking of hydrogel network and gum acacia used is biocompatible and readily available.

CONCLUSION

Gum acacia containing hydrogels were prepared and used as a dual-drug delivery system for antiprotozoal agents. The swelling ratio of the hydrogel networks was found to be influenced by the degree of cross-linking of gum acacia. The swelling ratio of the hydrogel networks decreased with an increase in the concentration of the gum acacia. These systems allowed the molecular dispersion of hydrophobic drugs in the hydrophilic network. The drugs release profiles proved that the addition of gum acacia, a natural occurring polymer to the hydrogel networks influenced the rate of release of the antiprotozoal agents from the hydrogels. The release kinetics of curcumin and *N*-(7-chloroquinolin-4-yl)propane-1,3-diamine from the hydrogels was found to correspond best with the Korsmeyer–Peppas release mechanism. *N*-(7-chloroquinolin-4-yl)propane-1,3-diamine exhibited a short term release while curcumin exhibited a long term sustained release in all the hydrogel network. The release profiles of both drugs followed a non-Fickian anomalous transport. These hydrogels are easy to prepare, exhibit different release profiles of the drugs, the release mechanism of the drugs can be controlled by varying the degree of cross-linking of gum acacia and hence are potential dual-drug delivery systems for effective combination therapy with extended therapeutic window.

ACKNOWLEDGMENTS

The financial assistance of the South African National Research Foundation (NRF) towards this research is hereby acknowledged.

REFERENCES

1. Wei, L.; Cai, C.; Lin, J.; Chen, T. *Biomaterials* **2009**, *30*, 2606.
2. Watanabe, M.; Kawano, K.; Toma, K.; Hattori, Y.; Maitani, Y. *J. Control. Release* **2008**, *127*, 231.
3. Aderibigbe, B. A.; Neuse, E. W.; Sadiku, E. R.; Shina Ray, S.; Smith, P. J. *J. Biomed. Mater. Res. Part A* **2013**, *102*, 1941.
4. Aderibigbe, B. A.; Neuse, E. W. *J. Inorg. Organomet. Polym. Mater.* **2012**, *22*, 429.
5. Nkazi, B. D.; Neuse, E. W.; Aderibigbe, B. A. *J. Inorg. Organomet. Polym. Mater.* **2012**, *22*, 886.
6. Hoffman, A. S. *Adv. Drug Deliv. Rev.* **2002**, *54*, 3.
7. Yannas, I. V.; Lee, E.; Orgill, D.; Skrabut, E. M.; Murphy, G. M. *PNAS* **1989**, *86*, 933.
8. Hubbell, J. A. *Curr. Opin. Solid State Mater. Sci.* **1998**, *3*, 246.
9. Kim, B. S.; Nikolovski, J.; Bonadio, J.; Mooney, D. J. *Nat. Biotech.* **1999**, *17*, 979.
10. Das, A.; Wadhwa, S.; Srivastav, A. K. *Drug Deliv.* **2006**, *13*, 139.
11. Nishi, K. K.; Antony, M.; Jayakrishnan, A. *J. Pharm. Pharmacol.* **2007**, *59*, 485.
12. Bhattarai, N.; Gunn, J.; Zhang, M. *Adv. Drug Deliv. Rev.* **2010**, *62*, 83.
13. Izydorczyk, M.; Cui, S. W.; Wang, Q. http://uqu.edu.sa/files2/tiny_mce/plugins/filemanager/files/4300270/1/2/1574_C006.pdf. Accessed 20 June 2013.
14. Gils, P. S.; Ray, D.; Sahoo, P. K. *Int. J. Biol. Macromol.* **2010**, *46*, 237.
15. Raghavendra, G. M.; Jayaramudu, T.; Varaprasad, K.; Sadiku, E. R.; Sinha Ray, S.; Mohana Rajua, K. *Carbohydr. Polym.* **2013**, *93*, 553.
16. Paulino, A. T.; Guilherme, M. R.; Mattoso, L. H. C.; Tambourgi, E. B. *Metal Contain. Metallo-Supramolecular Polym. Mater.* **2010**, *211*, 1196.
17. Juby, K. A.; Dwivedi, C.; Kumar, M.; Kota, S.; Misra, H. S.; Bajaj, P. N. *Carbohydr. Polym.* **2012**, *89*, 906.
18. Kaith, B. S.; Ranjta, S. *Desalin. Water Treat.* **2010**, *24*, 28.
19. Santos, M. C.; Guilherme, M. R.; Espires-Carrion, R. C.; Reis, A. V. <http://www.cifarp.com.br/cd2011/abstracts/NSP%20106%20-%20986.pdf>. Accessed 30 April 2014.
20. Dostelek, J.; Johas, U. *Adv. Eng. Appl. Sci.* **2012**, *1*, 5.
21. Han, Y. A.; Singh, M.; Saxen, B. B. *Contraception* **2007**, *76*, 132.
22. Fathollahiipur, S.; Maziarfar, S.; Tavakoli, J. Characterization and Evaluation of Acacia Gum Loaded PVA Hybrid Wound Dressing. *Biomedical Engineering (ICBME)*, 18–20 December 2013, 20th Iranian Conference, pp 149–154.
23. Malaria, WHO fact sheet No. 94. <http://www.who.int/mediacentre/factsheets/fs094/en/>. Accessed 26 August 2014.
24. Ward, S. A.; Bray, P. G.; Ritchie, G. Y. In *Drug Transport in Antimicrobial and Anticancer Chemotherapy*; Georgopapadakou, N. H. Ed.; Dekker: New York, **1995**; p 353–376.
25. Zaffanello, M.; Franchini, M.; Fanos, V. *Pharmacotherapy* **2008**, *28*, 125.
26. Cui, L.; Miao, J.; Cui, L. *Antimicrob. Agent Chemother.* **2007**, *51*, 488.
27. De, D.; Byers, L. D.; Krogstad, D. J. *J. Heterocycl. Chem.* **1997**, *34*, 315.
28. Madrid, P. B.; Wilson, N. T.; De Risi, J. L.; Guy, R. K. *J. Comb. Chem.* **2004**, *6*, 437.
29. Rojas, F. A.; Kouznetsov, V. V. *J. Braz. Chem. Soc.* **2011**, *22*, S1.
30. Krishna Mohan, P. R.; Sreelakshmi, G.; Muraleedharan, C. V.; Joseph, R. *Vib. Spectrosc.* **2012**, *62*, 77.
31. Rao, Y. N.; Banerjee, D.; Datta, A.; Das, S. K.; Guin, R.; Saha, A. *Radiat. Phys. Chem.* **2010**, *79*, 1240.
32. Gils, P. S.; Ray, D.; Mohanta, G. P.; Manavalan, R.; Sahoo, P. K. *Int. J. Pharm. Pharm. Sci.* **2009**, *1*, 43.
33. Lucht, L. M.; Peppas, N. A. *J. Appl. Polym. Sci.* **1987**, *33*, 1557.
34. Nagireddy, N. R.; Murali, M. Y.; Kokkarachedu, V.; Sakey, R.; Kanikireddy, V.; Alias, J. P.; Konduru, M. R. *J. Polym. Res.* **2011**, *18*, 2285.
35. Zohuriaan-Mehr, M. J.; Motazed, I. Z.; Kabiri, I. K.; Ershad-Langroudi, I. A.; Allahdadi, I. *J. Appl. Polym. Sci.* **2006**, *102*, 5667.
36. Raji, Z.; Kos, G.; Zorc, B.; Singh, P. P.; Singh, S. *Acta Pharm.* **2009**, *59*, 107.
37. Dandekar, P. P.; Jain, R.; Patil, S.; Dhumal, R.; Tiwari, D.; Sharma, S.; Vanage, G.; Patravale, V. *J. Pharm. Sci.* **2010**, *99*, 4992.
38. Nishi, K. K.; Jayakrishnan, A. *Biomacromolecules* **2007**, *8*, 84.
39. Ritger, P. L.; Peppas, N. A. *J. Control. Release* **1987**, *5*, 23.
40. Colombo, P.; Bettini, R.; Catellani, P. L.; Santi, P.; Peppas, N. A. *Eur. J. Pharm. Sci.* **1999**, *9*, 33.
41. Castro, E.; Mosquera, V.; Katime, I. *Nanomater. Nanotechnol.* **2012**, *2*, 1.
42. Perale, G.; Rossi, F.; Santoro, M.; Peviani, M.; Papa, S.; Llupi, D.; Torriani, P.; Micotti, E.; Previdi, S.; Cervo, L.; Sundström, E.; Boccaccini, A. R.; Masi, M.; Forloni, G.; Veglianes, P. *J. Control. Release* **2012**, *159*, 271.